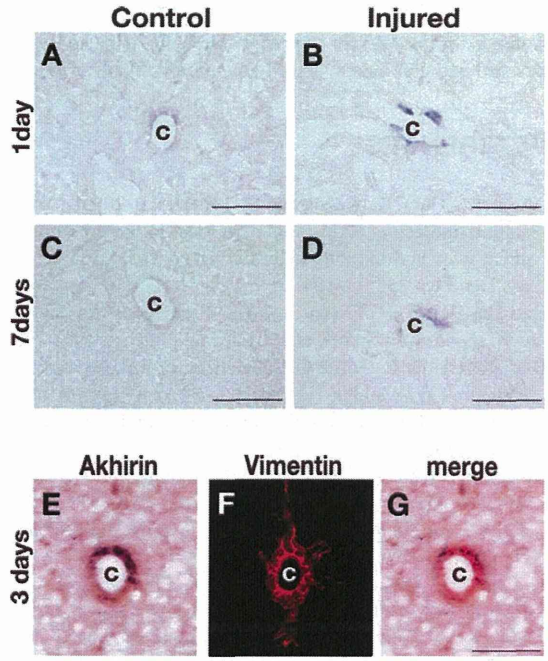

Figure 6 SCI induces *AKH* expression. (A–D): *AKH*+/+ mice at P30 were anesthetized and received laminectomies at spinal vertebrate. ISH was performed with *AKH* probe on day 1 (A, B) and day 7 (C, D) postinjury. Note that *AKH* expression is induced in the damaged spinal cord at the central canal. (E–G): ISH and immunohistochemistry were performed with *AKH* probe (E) and anti-Vimentin antibody (F) on day 3, respectively. Merge (G). Note that *AKH* expressing cells (purple signals in E) were overlapped with the Vimentin-positive ependymal cells (red signals in F) in the central canal (G). c, central canal. Bars: 100 μm. [Color figure can be viewed in the online issue, which is available at wileyonlinelibrary.com.]

The Cell Proliferation and Differentiation are Affected in *AKH* Mutant Mice

In this study, we show that the size of the neural tube was smaller in *AKH*−/− mice compared with *AKH*+/+ mice. One possible reason for the smaller size could be due to a significant reduction in the proliferative activity in the spinal cord of *AKH*−/− during development. Importantly, our experiments highlighted that the loss-of-function of *AKH* might have a role in regulating the proliferative activity in the mice spinal cord. To examine the difference in neurosphere formation between *AKH*+/+ and *AKH*−/− mice spinal cord, we cultured the dissociated cells and analyzed their size and number. Although the number of spheres is similar, the size of *AKH*−/− derived spheres is dramatically smaller than that of *AKH*+/+. This *in vitro* observation is consistent with the *in vivo* observation showing the reduced number of BrdU-uptake cells in *AKH*−/− spinal cord. To assess the involvement of *AKH* in the dorso-ventral patterning in the neural tube, we performed immunohistochemistry using Isl1/2, Pax6, GFAP, and Nestin, antibodies with *AKH*−/− and *AKH*+/+ spinal cords. We found that the total numbers of motoneurons and interneuron markers, Isl1/2-positive cells, were reduced in *AKH*−/− spinal cord. Interestingly, the loss-of-function of *AKH*−/− shows the reduction of Pax6 expression in the neural tube. Furthermore, the expression of the stem/progenitor cell markers, GFAP and Nestin, were reduced in *AKH*−/− mice spinal cord. Our experiments demonstrate that the *AKH* regulate the cell differentiation and proliferation during spinal cord development. The secreted morphogen Sonic hedgehog (Shh) is required for the cell-type specification and the proper formation of the ependymal zone during spinal cord development (Yu et al., 2013). As the expression of *AKH* and *Shh* is overlapped in the floor plate at E9.5, it would be interesting to examine the molecular interaction between AKH and Shh.

AKH Expression is Upregulated After SCI

It has been reported that, in the ependymal cell niche, ependymal cells of the spinal cord are normally quiescent in adult mice but after SCI they are rapidly activated, proliferative, and undergoes multilinage differentiation to contribute astrocytes to the injury tissue and display stem cells properties (Shihabuddin et al., 2000). Furthermore, ependymal cells contribute to the regeneration of oligodendrocytes and remyelination after SCI (Meletis et al., 2008). In this study, we showed that *AKH* expression is rapidly upregulated one day after an injury in adult mice. Next, we examined the distribution of Nestin and Vimentin in an injured spinal cord, as it was reported that the Nestin induction occurred within 48 h after injury in cells close to the central canal in the spinal cord (Frisén et al., 1995). The expression of Nestin and Vimentin were upregulated after 3 days of injury although we could not observe the differences between the control and injury sites a day after injury [data not shown]. Our data raises the possibility that AKH controls the cell proliferation and differentiation around the central canal as an immediate early response gene after injury.

The Distribution of Ependymal Cells, Astrocytes, and Proliferating Cells in *AKH*−/− Mice

A schematic view of the central canal niche in a mouse spinal cord provided here [Fig. 7] based on this work, may facilitate further investigation on the

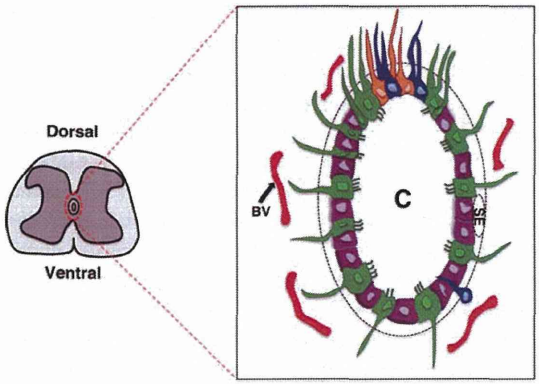

Figure 7 Schematic diagram of the mouse spinal cord ependymal cell niche. The central canal (c) in the spinal cord is lined with ependymal cells that express Vimentin (green). The neural stem cells and stem/progenitor cells present in the niche are represented by dorsal GFAP expressing astrocytes (blue) and Nestin expressing cells (orange), respectively. *AKH* expression in middle and ventral central canal can also be seen (purple). BV, blood vessel. SE, sub-ependymal layer. [Color figure can be viewed in the online issue, which is available at wileyonlinelibrary.com.]

important roles of *AKH* for regulating the stem cells in the intact and injured spinal cord. In this schematic, the neural stem cells and the neural stem/progenitor cells present in the niche are represented by GFAP- and Nestin-positive cells, respectively. Ependymal cells express Vimentin. AKH is mainly secreted from the middle and ventral central canal and it might be retained as a heterophilic adhesion molecule on the surface of neural stem/progenitor cells mediating the cell–cell interaction (Mothe and Tator, 2005). This study identifies a crucial role for AKH in regulating the proliferation and differentiation in the central canal of a mouse spinal cord.

CONCLUSION

In summary, we show that during development, a soluble molecule Akhirin, which belongs to VWA superfamily, is specifically expressed in the ependymal cells, which possess latent neural stem cell properties, of the central canal spinal cord. We demonstrate that the proliferation and differentiation of cells were affected *in vivo* and *in vitro* in *AKH−/−* mice. Furthermore, *AKH* expression in the central canal is upregulated in the injured spinal cord. Taken together, we provide a novel molecular mechanism for regulating the ependymal niche in the central canal by AKH.

We thank Drs. Campbell and Asrafuzzaman and all members of our labs for their valuable help. We also thank Drs. Shimamura, Esumi, and Mcmahon for cDNA probes.

REFERENCES

Ahsan M, Ohta K, Kuriyama S, Tanaka H. 2005. Novel soluble molecule, Akhirin, is expressed in the embryonic chick eyes and exhibits heterophilic cell-adhesion activity. Dev Dyn 233:95–104.

Barnabé-Heider F, Frisén J. 2008. Stem cells for spinal cord repair. Cell Stem Cell 3:16–24.

Barnabé-Heider F, Göritz C, Sabelström H, Takebayashi H, Pfrieger FW, Meletis K, Frisén J. 2010. Origin of new glial cells in intact and injured adult spinal cord. Stem Cell 7:470–482.

Bodega G, Suárez I, Rubio M. 1994. Ependyma: Phylogenetic evolution of glial fibrillary acidic protein (GFAP) and vimentin expression in vertebrate spinal cord. Histochemistry 102:113–122.

Crowe MJ, Bresnahan JC, Shuman SL, Masters JN, Beattie MS. 1997. Apoptosis and delayed degeneration after spinal cord injury in rats and monkeys. Nat Med 3: 73–76.

Edwards MA, Yamamoto M, Caviness VS. 1990. Organization of radial glia and related cells in the developing murine CNS. An analysis based upon a new monoclonal antibody marker. Neuroscience 36:121–144.

Ericson J, Thor S, Edlund T, Jessell TM, Yamada T. 1992. Early stages of motor neuron differentiation revealed by expression of homeobox gene Islet-1. Science 256:1555–1560.

Frisén J, Johansson CB, Török C, Risling M, Lendahl U. 1995. Rapid, widespread, and longlasting induction of nestin contributes to the generation of glial scar tissue after CNS injury. J Cell Biol 131:453–464.

Fu H, Qi Y, Tan M, Cai J, Takebayashi H, Nakafuku M, Richardson W, Qiu M. 2002. Dual origin of spinal oligodendrocyte progenitors and evidence for the cooperative role of Olig2 and Nkx2.2 in the control of oligodendrocyte differentiation. Development 129:681–693.

Fujimoto Y, Abematsu M, Falk A, Tsujimura K, Sanosaka T, Juliandi B, Semi K, Namihira M, Komiya S, Smith A, Nakashima K. 2012. Treatment of a mouse model of spinal cord injury by transplantation of human induced pluripotent stem cell-derived long-term self-renewing neuroepithelial-like stem cells. Stem Cells 30:1163–1173.

Gerdes J, Schwab U, Lemke H. 1983. Production of a mouse monoclonal antibody reactive with a human nuclear antigen associated with cell proliferation. Int J Cancer 31:13–20.

Goulding MD, Lumsden A, Gruss P. 1993. Signals from the notochord and floor plate regulate the region-specific expression of two Pax genes in the developing spinal cord. Development 117:1001–1016.

Grossman S. 2001. Temporal–spatial pattern of acute neuronal and glial loss after spinal cord contusion. Exp Neurol 168:273–282.

Hamilton LK, Truong MKV, Bednarczyk MR, Aumont A, Fernandes KJL. 2009. Cellular organization of the central canal ependymal zone, a niche of latent neural stem cells in the adult mammalian spinal cord. NSC 164:1044–1056.

Horky LL, Galimi F, Gage FH, Horner PJ. 2006. Fate of endogenous stem/progenitor cells following spinal cord injury. J Comp Neurol 498:525–538.

Hugnot JP. 2010. The spinal cord neural stem cell niche. In: Sun T, editor. Neural Stem Cells and Therapy. Intech, pp 71–92.

Hugnot JP, Franzen R. 2011. The spinal cord ependymal region: A stem cell niche in the caudal central nervous system. Front Biosci (Landmark Ed) 16:1044–1059.

Johansson CB, Momma S, Clarke DL. 1999. Identification of a neural stem cell in the adult mammalian central nervous system. Cell 96:25–34.

Kinameri E, Inoue T, Aruga J, Imayoshi I, Kageyama R, Shimogori T, Moore AW. 2008. Prdm proto-oncogene transcription factor family expression and interaction with the Notch-Hes pathway in mouse neurogenesis. PLoS One 3:e3859.

Kojima A, Tator CH. 2002. Intrathecal administration of epidermal growth factor and fibroblast growth factor 2 promotes ependymal proliferation and functional recovery after spinal cord injury in adult rats. J Neurotrauma 19:223–238.

Liang X, Song M-R, Xu Z, Lanuza GM, Liu Y, Zhuang T, Chen Y, Pfaff SL, Evans SM, Sun Y. 2011. Isl1 is required for multiple aspects of motor neuron development. Mol Cell Neurosci 47:215–222.

Lukaszewicz AI, Anderson DJ. 2011. Cyclin D1 promotes neurogenesis in the developing spinal cord in a cell cycle-independent manner. Proc Natl Acad Sci USA 108: 11632–11637.

Meletis K, Barnabé-Heider F, Carlén M, Evergren E, Tomilin N, Shupliakov O, Frisén J. 2008. Spinal cord injury reveals multilineage differentiation of ependymal cells. PLoS Biol 6:e182.

Mothe A, Tator C. 2005. Proliferation, migration, and differentiation of endogenous ependymal region stem/progenitor cells following minimal spinal cord injury in the adult rat. Neuroscience 131:177–87.

Namiki J, Tator CH. 1999. Cell proliferation and nestin expression in the ependyma of the adult rat spinal cord after injury. J Neuropathol Exp Neurol 58:489–498.

Okada S, Nakamura M, Katoh H, Miyao T, Shimazaki T, Ishii K, Yamane J, Yoshimura A, Iwamoto Y, Toyama Y, Okano H. 2006. Conditional ablation of Stat3 or Socs3 discloses a dual role for reactive astrocytes after spinal cord injury. Nat Med 12:829–834.

Sabourin J-C, Ackema KB, Ohayon D, Guichet P-O, Perrin FE, Garces A, Ripoll C, Charité J, Simonneau L, Kettenmann H, Zine A, Privat A, Valmier J, Pattyn A, Hugnot J-P. 2009. A mesenchymal-like ZEB1(+) niche harbors dorsal radial glial fibrillary acidic protein-positive stem cells in the spinal cord. Stem Cells 27:2722–2733.

Shihabuddin LS, Horner PJ, Ray J, Gage FH. 2000. Adult spinal cord stem cells generate neurons after transplantation in the adult dentate gyrus. J Neurosci 20: 8727–35.

Tanabe Y, Jessell TM. 1996. Diversity and pattern in the developing spinal cord. Science 274:1115–1123.

Weiss S, Dunne C, Hewson J, Wohl C, Wheatley M, Peterson AC, Reynolds BA. 1996. Multipotent CNS stem cells are present in the adult mammalian spinal cord and ventricular neuroaxis. J Neurosci 16:7599–7609.

Yasuda A, Tsuji O, Shibata S, Nori S, Takano M, Kobayashi Y, Takahashi Y, Fujiyoshi K, Hara CM, Miyawaki A, Okano HJ, Toyama Y, Nakamura M, Okano H. 2011. Significance of remyelination by neural stem/progenitor cells transplanted into the injured spinal cord. Stem Cells 29:1983–1994.

Yu K, McGlynn S, Matise MP. 2013. Floor plate-derived sonic hedgehog regulates glial and ependymal cell fates in the developing spinal cord. Development 140: 1594–1604.

nature COMMUNICATIONS

ARTICLE

Received 26 Apr 2014 | Accepted 4 Feb 2015 | Published 9 Mar 2015

DOI: 10.1038/ncomms7514 OPEN

TLR9 signalling in microglia attenuates seizure-induced aberrant neurogenesis in the adult hippocampus

Taito Matsuda[1], Naoya Murao[1,2], Yuki Katano[1,2], Berry Juliandi[1,3], Jun Kohyama[4], Shizuo Akira[5,6], Taro Kawai[7] & Kinichi Nakashima[1]

Pathological conditions such as epilepsy cause misregulation of adult neural stem/progenitor populations in the adult hippocampus in mice, and the resulting abnormal neurogenesis leads to impairment in learning and memory. However, how animals cope with abnormal neurogenesis remains unknown. Here we show that microglia in the mouse hippocampus attenuate convulsive seizure-mediated aberrant neurogenesis through the activation of Toll-like receptor 9 (TLR9), an innate immune sensor known to recognize microbial DNA and trigger inflammatory responses. We found that microglia sense self-DNA from degenerating neurons following seizure, and secrete tumour necrosis factor-α, resulting in attenuation of aberrant neurogenesis. Furthermore, TLR9 deficiency exacerbated seizure-induced cognitive decline and recurrent seizure severity. Our findings thus suggest the existence of bidirectional communication between the innate immune and nervous systems for the maintenance of adult brain integrity.

[1] Department of Stem Cell Biology and Medicine, Graduate School of Medical Sciences, Kyushu University, 3-1-1 Maidashi, Higashi-ku, Fukuoka 812-8582, Japan. [2] Laboratory of Gene Regulation Research, Graduate School of Biological Sciences, Nara Institute of Science and Technology (NAIST), Nara 630-0192, Japan. [3] Department of Biology, Bogor Agricultural University, Bogor 16144, Indonesia. [4] Department of Physiology, School of Medicine, Keio University, 35 Shinanomachi, Shinjuku-ku, Tokyo 160-8582, Japan. [5] Laboratory of Host Defense, World Premier International Immunology Frontier Research Center, Osaka University, Osaka 565-0871, Japan. [6] Department of Host Defense, Research Institute for Microbial Diseases, Osaka University, Osaka 565-0871, Japan. [7] Laboratory of Molecular Immunobiology, Graduate School of Biological Sciences, NAIST, Nara 630-0192, Japan. Correspondence and requests for materials should be addressed to K.N. (email: kin1@scb.med.kyushu-u.ac.jp).

Adult neural stem/progenitor cells (aNS/PCs) in the subgranular zone (SGZ) of the adult hippocampal dentate gyrus (DG) proliferate and give rise to new neurons continuously throughout life to maintain proper brain functions[1]. Although this homoeostatic neurogenesis is strictly controlled under normal physiological conditions, misregulation of aNS/PCs leads to aberrant neurogenesis and impairment of hippocampal-dependent learning and memory under pathological conditions such as stress, depression, ischaemia and epilepsy[2]. The aNS/PC niche, a microenvironment comprising various components including blood vessels, neurons, astrocytes and microglia, is known to contribute to different aspects of neurogenesis under both normal and pathological conditions[2–7]. However, how it responds to pathological conditions to rectify any aberrant behaviour of aNS/PCs is yet to be elucidated.

Microglia, the major immune cell type in the brain, remove dying cells and cellular debris without inducing inflammation under physiological conditions[8]. In response to pathological insults such as infection or brain injury, activated microglia accumulate in the injured site and secrete pro- and/or anti-inflammatory cytokines[9,10]. In addition to these functions, increasing evidence suggests that microglia play important roles in aNS/PC regulation under physiological conditions[11–13].

Toll-like receptors (TLRs) are innate immune receptors that recognize pathogen- or damage-associated molecular patterns (P/DAMPs)[14–16], and provide an important machinery by which microglia can sense both pathogen- and host-derived ligands and consequently secrete pro- and/or anti-inflammatory cytokines. While TLR2 and TLR4 have been implicated in adult hippocampal neurogenesis under physiological conditions[17], it is completely unknown whether the nucleic acid-sensing TLR7 and TLR9 can also regulate neurogenesis. To elucidate the functions of these TLRs is important, particularly in pathological conditions, because nucleic acids released from endogenous damaged cells could activate them, resulting in the misregulation of aNS/PC behaviour.

We report here that the loss of TLR9 but not TLR7 reduced seizure-mediated sustained microglial activation and tumour necrosis factor-alpha (TNF-α) production in the hippocampus. Pharmacological inhibition of microglial activation or TNF-α production in wild-type (WT) mice exacerbated aberrant neurogenesis to a similar extent to that observed in TLR9 knockout (KO) mice after seizure. Furthermore, conditioned medium (CM) from hyperactivated hippocampal neurons upregulated *Tnf-α* expression in primary cultures of WT but not TLR9 KO microglia, and this effect was completely abolished when the CM was pretreated with DNase. These results indicate that microglia are activated through TLR9 signalling triggered by self-DNA derived from seizure-induced degenerating neurons in the hippocampus, leading to a sustained expression of TNF-α which attenuates the induced aberrant neurogenesis.

Results

TLR9 deficiency aggravates aberrant neurogenesis. We found that Iba1-positive microglia were in close proximity to about 80% of aNS/PCs (positive both for green fluorescent protein (GFP) expressed under the promoter of the NS/PC marker gene *Sox2* and for the aNS/PC marker glial fibrillary acidic protein (GFAP)) in the SGZ of the hippocampus under both physiological and pathological conditions (Supplementary Fig. 1a–c), implying that niche-resident microglia activated in response to pathological insults also affect the behaviour of aNS/PCs by producing pro- and/or anti-inflammatory cytokines.

As a first step towards understanding the roles of TLR7 and TLR9, we confirmed their expression in microglia and found that they are much more highly expressed in these cells than in other neural cell types including NSCs (Supplementary Fig. 1d). To investigate the role of TLR7 and TLR9 in adult hippocampal neurogenesis, we injected bromodeoxyuridine (BrdU) once a day for 7 days into physiologically normal 8-week-old WT, TLR7-KO and TLR9-KO mice to label proliferating aNS/PCs in the DG and killed the mice 1 day after the final injection. We observed no significant difference among these mice (Fig. 1a–c), since TLR signalling is activated by P/DAMPs only under pathological conditions[15,16]. Although we have previously reported that convulsive seizure induces aberrant neurogenesis in the adult DG[18], how animals respond to this pathological condition remains unknown. We thus sought to examine the effects of TLR7 and TLR9 deficiency on the response to convulsive seizure induction. To induce the seizure, we administered kainic acid (KA), a potent glutamate analogue that triggers neuronal

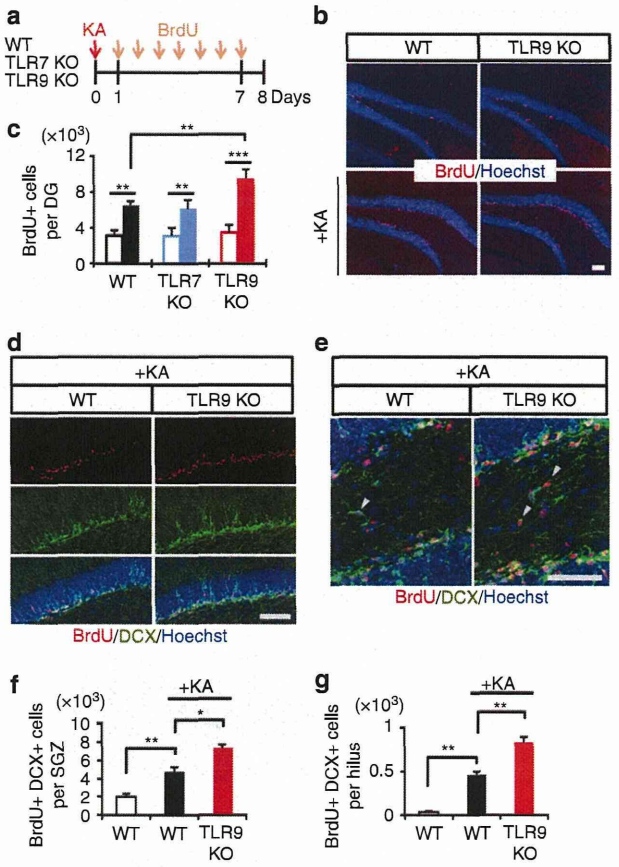

Figure 1 | TLR9 deficiency aggravates seizure-induced aberrant neurogenesis. (**a**) Experimental timeline for assessing aNS/PC proliferation in WT, TLR7-KO and TLR9-KO mice. (**b**) Representative images of the DG and stained with BrdU (red) and Hoechst (blue) showed that KA-induced proliferation of aNS/PCs in TLR9-KO mice was more extensive than in WT mice. Scale bar, 50 μm. (**c**) Quantification of total number of BrdU-positive (BrdU+) cells in the DG with (filled bars) or without (open bars) KA treatment. After seizure, the number of BrdU+ cells was higher in TLR9-KO mice than in WT mice ($n=5$ animals). (**d**,**e**) Representative images of BrdU (red) and DCX (green) double-labelled (BrdU+DCX+) newly generated neurons in the SGZ (**d**) and the hilus (**e**) ($n=5$ animals). Scale bars, 50 μm. White arrowheads indicate new neurons located ectopically in the hilus. (**f**,**g**) Quantification of the number of BrdU+DCX+ cells in **c** (SGZ, **f**) and **e** (hilus, **g**; $n=5$ animals). $^{*}P<0.05$, $^{**}P<0.01$ and $^{***}P<0.001$ by analysis of variance with Tukey *post-hoc* tests.

hyperactivation, intraperitoneally to WT, TLR7-KO and TLR9-KO mice. KA-induced acute convulsive seizure is known to trigger aberrant augmentation of neurogenesis in the DG and the migration of newborn neurons to ectopic locations such as the hilus, resulting in the impairment of hippocampus-dependent memory[3,18,19]. Consistent with previous reports, we observed a significant increase in the number of BrdU-positive cells within the SGZ in all KA-treated mice (Fig. 1a–c). Interestingly, while the number of BrdU-positive cells within the SGZ at 1 week after KA administration did not differ between WT and TLR7-KO mice, the number was higher in TLR9-KO mice (Fig. 1a–c). In addition, an increased number of BrdU-retaining and doublecortin (DCX, an immature neuron marker)-expressing newly generated and immature neurons was observed in the DG, including both the SGZ and the hilus, of TLR9-KO mice (Fig. 1d–g), suggesting that the loss of TLR9 stimulates KA-induced aberrant neurogenesis. We decided to focus on TLR9-KO mice in the following experiments because neurogenesis in TLR7-KO mice was indistinguishable from that in WT mice even in the pathological condition.

We further traced the differentiation and survival of newly generated cells in the DG at 3 weeks after the last BrdU injection (Fig. 2a). The TLR9-KO mice showed a higher number of BrdU-retaining cells in the DG than that in WT mice (Fig. 2b,d), and the majority of BrdU-retaining cells had become positive for the mature neuronal marker NeuN (Fig. 2b–e). However, the loss of TLR9 had no effect on the proportion of NeuN-positive neurons among BrdU-positive cells. Concordant with the increase in BrdU-positive cells, the number of newly generated S100β- or GFAP-positive astrocytes also increased in the DG of TLR9-KO compared with WT mice (Fig. 2b–e), suggesting that aNS/PC differentiation *per se* was not affected by the loss of TLR9 as shown in Fig. 2f for neuronal differentiation as an example. Furthermore, we measured the proportion of surviving total BrdU-positive cells in WT and TLR9-KO mice. To calculate the ratio of surviving cells after seizure, we divided the total number of BrdU-positive cells at 3 weeks after the last BrdU injection by that at 1 day after the last BrdU injection. We found no difference in the survival ratio (Fig. 2g), indicating that TLR9 signalling does not contribute to the survival of newborn cells in the DG. Taken together, these results suggest that TLR9 deficiency aggravates seizure-induced aberrant neurogenesis in the hippocampus by promoting aNS/PC proliferation. In other words, these data indicate that TLR9 signalling attenuates seizure-induced abnormal proliferation of aNS/PCs to maintain homoeostatic neurogenesis in the DG.

Activated microglia attenuates aberrant neurogenesis. Before further analyzing TLR9 function, we determined whether TLR9 is indeed expressed in microglia in the DG *in vivo*. As shown in Supplementary Fig. 1e, Iba1-positive microglia clearly expressed TLR9. We also examined whether i.p. KA injection compromises the integrity of the blood–brain barrier (BBB) by using Evans blue dye, because macrophages infiltrate the damaged brain in conditions such as ischaemia through a disrupted BBB. However, Evans blue dye leakage was not found in the brain, while the dye was detected in other organs in both WT and TLR9-KO mice, indicating that the BBB remains intact after KA injection in these mice (Supplementary Fig. 1f). Although we cannot completely exclude the possibility that macrophages infiltrate the brain after seizure through the intact BBB, any such macrophage population would be exceedingly small compared with the brain-resident microglia. We therefore focused mainly on microglia as TLR9-expressing cells in this study.

Since it has been shown that epileptic seizure induces microglial activation in the hippocampus[20], we evaluated the microglial activation status in WT and TLR9-KO DG after seizure by immunohistochemistry with an antibody against CD68, which is upregulated in activated microglia (Supplementary Fig. 2a,b). Many CD68-positive activated microglia were detected in WT mice 7 days after seizure, whereas the activation was much lower

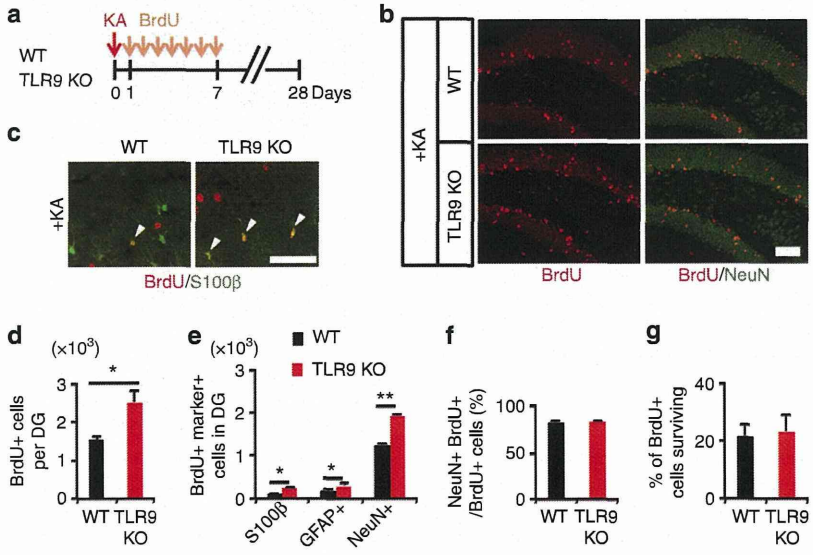

Figure 2 | Loss of TLR9 increases newly generated mature neurons after seizure. (**a**) Experimental scheme for examining the number of newly generated mature neurons. (**b**) Representative images of staining for NeuN (green) and BrdU (red) in the DG ($n=5$ animals). Scale bar, 50 μm. (**c**) Representative images of BrdU (red) and S100β (green) staining in the DG of KA-administered WT and TLR9-KO mice. White arrowheads indicate BrdU and S100β double-labelled newborn astrocytes. Scale bar, 50 μm. (**d**,**e**) The DG of TLR9 KO mice exhibited increased numbers of BrdU+ cells (**d**) and newly generated BrdU+NeuN+ mature neurons (**e**) ($n=5$ animals). (**f**,**g**) Quantification of BrdU+ cells for assessing differentiation (**f**) and survival (**g**) of newly generated cells in the DG ($n=5$ animals). (**d**) $^{*}P<0.05$ by Student's *t*-test. (**e**) $^{*}P<0.05$ and $^{**}P<0.01$ by analysis of variance with Tukey *post-hoc* tests.

in TLR9-KO mice, indicating that sustained microglial activation in the DG requires functional TLR9 (Fig. 3a). This result prompted us to ask whether TLR9-mediated microglial activation inhibits aNS/PC proliferation. To induce microglial activation, we prepared primary cultured microglia (Supplementary Fig. 3a) and stimulated them *in vitro* with the TLR9 ligand ODN1585. Incubation of microglia with ODN1585 upregulated the expression of two well-known targets of TLR signalling, *Tnf-α* and *Interferon* (*Ifn*) β, in a dose-dependent manner (Supplementary Fig. 3b). We then tested whether the CM of microglia activated with ODN1585 affects aNS/PC proliferation, and found that it decreased aNS/PC proliferation compared with control CM without affecting cell survival (Fig. 3b–d). We also performed experiments using different ligands (ODN2395 and ODN1826) for TLR9, and found that CM from microglia activated with these two ligands likewise inhibited aNS/PC proliferation (Supplementary Fig. 4). These data indicate that microglia activated through TLR9 inhibit aNS/PC proliferation *in vitro*.

Minocycline, a semisynthetic tetracycline derivative, is known to inhibit microglial activation *in vivo*[21]. To inhibit sustained microglial activation after seizure, we injected minocycline intraperitoneally into WT and TLR9-KO mice once daily for 8 consecutive days. We confirmed that seizure-induced microglial activation was inhibited by minocycline treatment (Supplementary Fig. 2b). When we inhibited microglial activation with minocycline in KA-administered WT mice, seizure-induced aberrant neurogenesis was exacerbated, reaching a level similar to

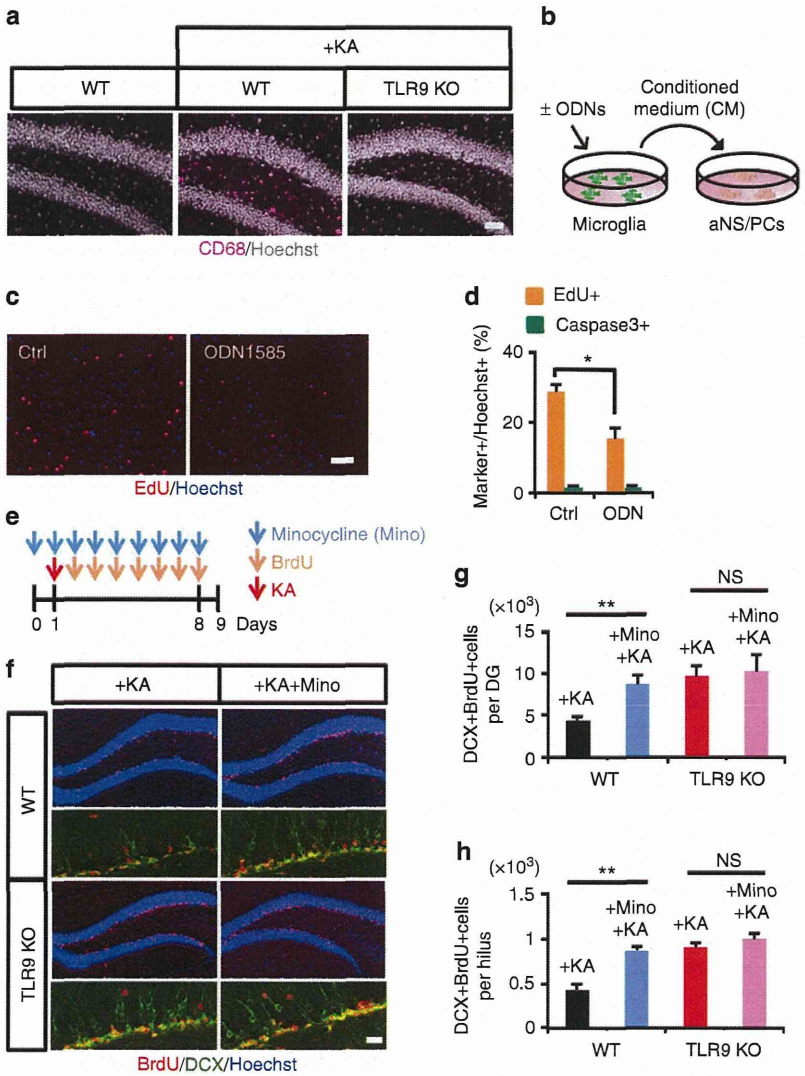

Figure 3 | Activated microglia attenuates aberrant neurogenesis. (**a**) Representative images of CD68+ (magenta) activated microglia in the DG of TLR9 KO and WT mice with or without KA treatment ($n=4$ animals). Scale bar, 50 μm. (**b**) Experimental scheme for assessing aNS/PC proliferation in the presence or absence of CM derived from ODN1585-stimulated microglia. (**c**) Representative images of EdU (red) and Hoechst (blue) staining of aNS/PCs cultured with CM of ODN1585-treated (right) and untreated (left) microglia as a control (Ctrl) ($n=5$ experiments). Scale bar, 50 μm. (**d**) Quantification of EdU + Hoechst + cells or an apoptotic cell marker active caspase3 + Hoechst + cells. ODN1585-dependent microglial activation inhibits aNS/PCs without affecting cell survival ($n=5$ experiments). (**e**) Experimental scheme for assessing aNS/PC proliferation in minocycline-treated mice. (**f**) Representative images of BrdU+ (red) DCX+ (green) newly generated neurons in the DG. Scale bar, 50 μm. (**g**,**h**) Quantification of the number of BrdU + DCX+ cells in the DG (**g**) and hilus (**h**) ($n=5$ animals). Ectopic neurogenesis increased in minocycline-treated mice to a similar extent to that observed in TLR9 KO mice ($n=5$ animals). (**d**) $^{*}P<0.01$ by Student's *t*-test. (**g**,**h**) NS means not significant ($P>0.05$). $^{*}P<0.05$, $^{**}P<0.01$ by analysis of variance with Tukey *post-hoc* tests.

that observed in TLR9-KO mice treated with KA alone (Fig. 3e–h). Furthermore, there were no differences in the number of BrdU- and DCX-positive cells (newly generated neurons) between minocycline-treated or -untreated TLR9-KO mice after seizure (Fig. 3f–h). Taken together, these results suggest that activated microglia attenuate seizure-induced neurogenesis through TLR9 signalling. Minocycline itself did not affect neurogenesis under normal physiological conditions (Supplementary Fig. 2c–e).

Microglia-derived TNF-α alleviates aberrant neurogenesis. Recent studies have shown that various inflammation-related molecules regulate adult neurogenesis in the DG[22–24], leading us to hypothesize that such molecules released from activated microglia might attenuate aberrant neurogenesis induced by seizure. To test this, we performed quantitative real-time PCR (qRT–PCR) analysis. At one day after seizure induction, expression of inflammatory cytokines, such as *Il-1β*, *Il-6* and *Tnf-α*, in both WT and TLR9-KO DG was upregulated compared to KA-untreated controls (Fig. 4a and Supplementary Fig. 5). Intriguingly, the higher expression level of *Tnf-α* and not other mRNAs was sustained in KA-treated WT mice at 4 or 7 days after seizure, yet the *Tnf-α* expression level in TLR9-KO mice reverted to the control level by 4 days after seizure induction (Fig. 4a). Given that TNF-α has previously been shown to suppress neurogenesis in the DG[23], we tested whether TNF-α inhibits aNS/PC proliferation *in vitro*, and found that it did so in a dose-dependent manner (Supplementary Fig. 6a,b). We also examined whether IL-12 and IFN-γ inhibit aNS/PC proliferation, because their expression differed between WT and TLR9-KO mice at day 1 after seizure (Supplementary Fig. 5). However, we found no difference in the number of EdU (a thymidine analogue)-positive cells irrespective of IL-12 and IFN-γ treatment, suggesting that aNS/PC proliferation is unaffected by these cytokines (Supplementary Fig. 6c–f). Therefore, we decided to focus on TNF-α in subsequent experiments. To examine whether TLR9 signalling-mediated TNF-α production by microglia inhibits aNS/PC proliferation, we pretreated CM samples from microglia with a TNF-α-neutralizing antibody or immunoglobulin-G (IgG) control, and added them to aNS/PC cultures (Fig. 4b). ODN1585-untreated microglial CM pretreated with the TNF-α antibody did not affect aNS/PC proliferation. In marked contrast, the anti-proliferative effect of the CM from ODN1585-treated microglia was abolished with the TNF-α antibody, indicating that TLR9 stimulation-induced TNF-α is the factor responsible for the inhibition of aNS/PC proliferation (Fig. 4c,d).

Thalidomide is known as a BBB-permeable inhibitor of TNF-α production[25]. To allow administered thalidomide enough time to be fully effective in inhibiting *Tnf-α* expression by the time of KA injection, we started the injection of thalidomide into WT mice 1 day before the KA injection, and continued once daily until 3 days after seizure; the mice were then killed 4 days after seizure. As shown in Supplementary Fig. 6g,h, we found that thalidomide treatment suppressed *Tnf-α* expression in the DG of WT mice 4 days after seizure. When we injected thalidomide into WT mice once daily for 8 consecutive days, in accordance with our *in vitro* experiments, suppression of TNF-α production aggravated aberrant neurogenesis *in vivo* as observed in thalidomide-untreated TLR9-KO mice after seizure (Fig. 4e–h).

Next, to understand more precisely the behaviour of aNS/PCs in response to seizure, we examined aNS/PC proliferation at earlier time points after KA administration in both WT and TLR9-KO mice. After 1, 2, 3 and 4 days of KA administration, we injected BrdU into these mice every 4 h (four times) and killed them 12 h after the last BrdU injection (Supplementary Fig. 7a). We found that the number of BrdU-positive cells which were proliferating at day 4 after seizure induction in WT mice was significantly higher than in untreated WT mice (Supplementary Fig. 7b,d). In contrast, statistically different BrdU-positive cell numbers between untreated and KA-treated mice were already observed at day 2 in TLR9-KO mice (Supplementary Fig. 7b,d). Moreover, these trends of increased BrdU-positive cell numbers in WT and TLR9-KO mice were inversely correlated with the degree of microglial activation and *Tnf-α* expression in these mice (Supplementary Fig. 7c,e). As shown in Supplementary Fig. 7e, a dramatic upregulation of *Tnf-α* expression in both WT and KO mice was observed at day 1 after KA injection, probably attributable to a direct effect of KA. By 2 days, *Tnf-α* expression in KA-injected TLR9-KO mice had already reverted to a level similar to that in the control, but was still high in KA-injected WT mice, suggesting that the difference was attributable to TLR9 deficiency. To confirm the effectiveness of thalidomide on the inhibition of *Tnf-α* expression, we then injected thalidomide into WT mice 1 day before the difference in *Tnf-α* expression between WT and TLR9 KO mice became apparent (day 2) (Supplementary Fig. 8a). As shown in Supplementary Figs 7d and 8c, BrdU-positive cells had not yet increased in response to KA treatment at day 3 in WT mice, but we did observe an increase of BrdU-positive cells in response to thalidomide treatment (Supplementary Fig. 8b,c). We then examined whether TNF-α reduces exacerbated neurogenesis in TLR9-KO mice after seizure. We infused recombinant TNF-α protein into the DG of TLR9-KO mice after seizure (Supplementary Fig. 9a) and found that TNF-α indeed reduced the seizure-induced aberrant neurogenesis in these mice (Supplementary Fig. 9b,c). Taken together, these results indicate that TLR9 signal-regulated TNF-α production by microglia is a critical process to withstand the aberrant neurogenesis following seizure.

TLR9 signalling does not affect localization of new neurons. Having shown that TLR9-dependent TNF-α production in microglia attenuates seizure-induced aNS/PC proliferation and ectopic generation of new neurons, we next asked whether TLR9 signalling affects the location of DCX-positive newly generated neurons in the DG at 8 days after seizure. The loss of TLR9 had no effect on the distribution of DCX-positive neurons, whereas the number of DCX-positive neurons in each area examined was increased in TLR9-KO mice after seizure compared with WT mice (Supplementary Fig. 10a–c). Since microglia activation and TNF-α production are important processes downstream of TLR9 signalling, minocycline and thalidomide treatment did not affect the distribution but did increase the number of DCX-positive cells, similar to TLR9 loss (Supplementary Fig. 10b). We also examined the morphology of DCX-positive cells after seizure by Sholl analysis and measurement of dendrite length. TLR9-KO mice showed no significant differences in these analyses, although KA itself affected the morphology of DCX-positive neurons (Supplementary Fig. 11a–c). Thus, these data indicate that TLR9 deficiency aggravates seizure-induced aberrant neurogenesis in the hippocampus by promoting aNS/PC proliferation.

Loss of TLR9 worsens seizure-induced behavioural impairments. We have previously shown that seizure-induced aberrant neurogenesis impairs a hippocampal-dependent cognitive function[18]. Since seizure-induced aberrant neurogenesis is exacerbated in TLR9-KO mice, we examined whether KA-treated TLR9-KO mice show further cognitive decline by subjecting KA-treated or -untreated WT and TLR9-KO mice to a hippocampus-dependent place recognition task (Fig. 5a). Administration of KA to WT mice induced cognitive decline in agreement with our previous

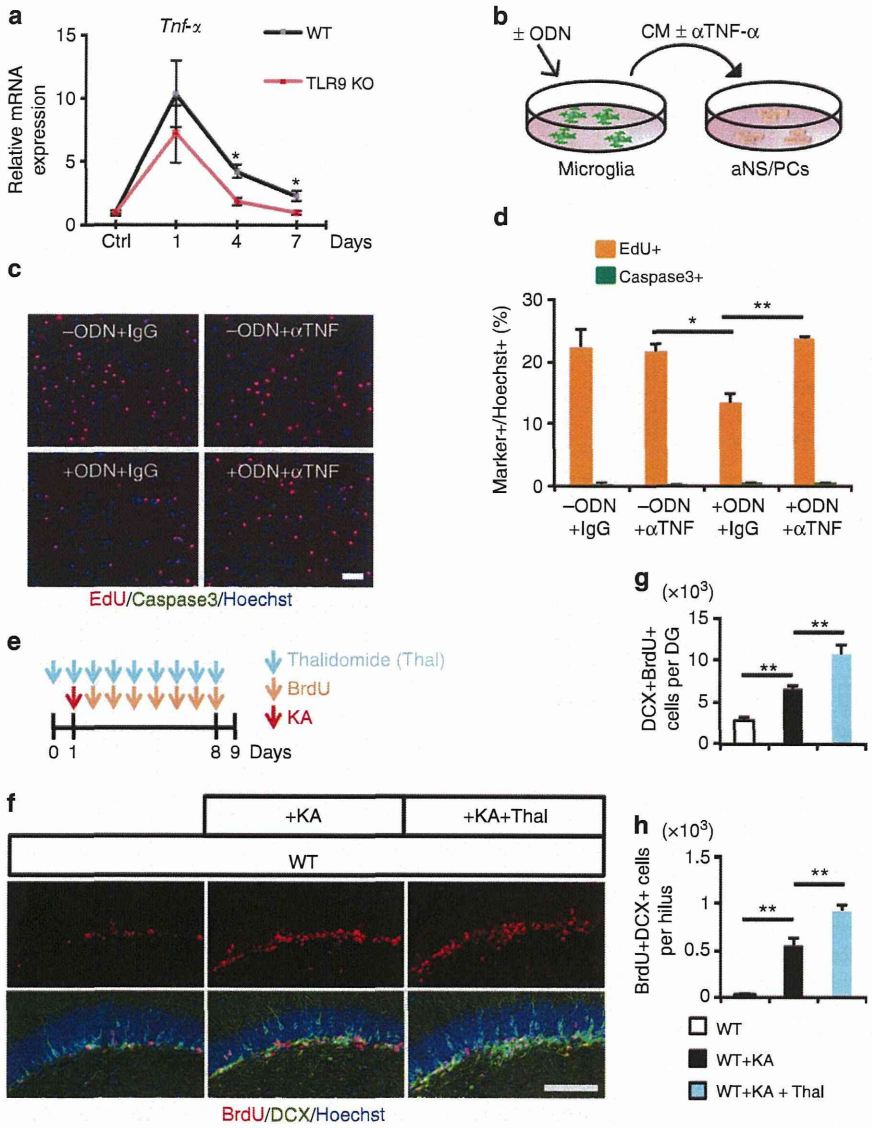

Figure 4 | Microglia-derived TNF-α alleviates aberrant neurogenesis. (**a**) qRT-PCR analyses of *Tnf-α* levels in the DG of WT and TLR9 KO mice at the indicated time points after seizure. Experimental controls were KA-untreated WT and TLR9 KO mice, respectively ($n=3$ animals). $^{*}P<0.05$ by analysis of variance (ANOVA) with Tukey *post-hoc* tests. (**b**) Experimental scheme for assessing aNS/PC proliferation in microglia culture-derived CM pretreated with TNF-α-neutralizing antibody or IgG control. (**c**) Representative images of EdU (red), active caspase3 (green) and Hoechst (blue) staining in aNS/PCs cultured with the indicated CM from microglia ($n=4$ experiments). Scale bar, 50 μm. (**d**) Quantification of EdU+ or active caspase3+ cells in **c** ($n=4$ experiments). (**e**) Experimental timeline for assessing aNS/PC proliferation in thalidomide (Thal)-treated mice. (**f**) Representative images of BrdU+DCX+ newly generated immature neurons in the DG ($n=4$ animals). Scale bar, 50 μm. (**g**,**h**) Quantification of the number of BrdU+DCX+ cells in **f**, in the DG (**g**) and in the hilus (**h**) ($n=4$ animals). $^{*}P<0.05$ and $^{**}P<0.01$ by ANOVA with Tukey *post-hoc* tests.

report[18] (Fig. 5b). Moreover, the loss of TLR9 aggravated this seizure-induced cognitive decline, although without KA treatment WT and TLR9-KO mice showed no significant difference in the test (Fig. 5b). When we inhibited microglial activation in WT mice treated with KA using minocycline, the level of impairment in these mice decreased to an extent similar to that observed in TLR9-KO mice without treatment (Fig. 5b). These data suggest that TLR9-mediated microglial activation attenuates seizure-induced cognitive decline in WT mice.

A recent study has indicated that ectopically located new neurons contribute to epileptogenesis[26]. This observation prompted us to examine whether either TLR9 deficiency or inhibition of microglia activation by minocycline affect the severity of seizure induced by KA re-injection at 48 days after the first KA injection (Fig. 5c). All mice showed no difference in scores of seizure following the first KA injection (Fig. 5d,e). Furthermore, the first administration of KA at low concentration did not affect the scores in WT or TLR9-KO mice (Supplementary Fig. 12a,b). However, when we re-injected KA at low concentration to TLR9-KO mice 48 days after the first KA injection, they developed more severe seizures compared with WT mice (Fig. 5f,g). Minocycline treatment indeed aggravated the symptoms in WT mice, *albeit* to a lesser extent than that observed in TLR9 KO mice without minocycline, probably because we ceased minocycline treatment at 7 days after the first KA injection. During the 7 days after the first KA administration, microglial activation was inhibited by minocycline, but resumed after the cessation of this treatment. We therefore inferred that

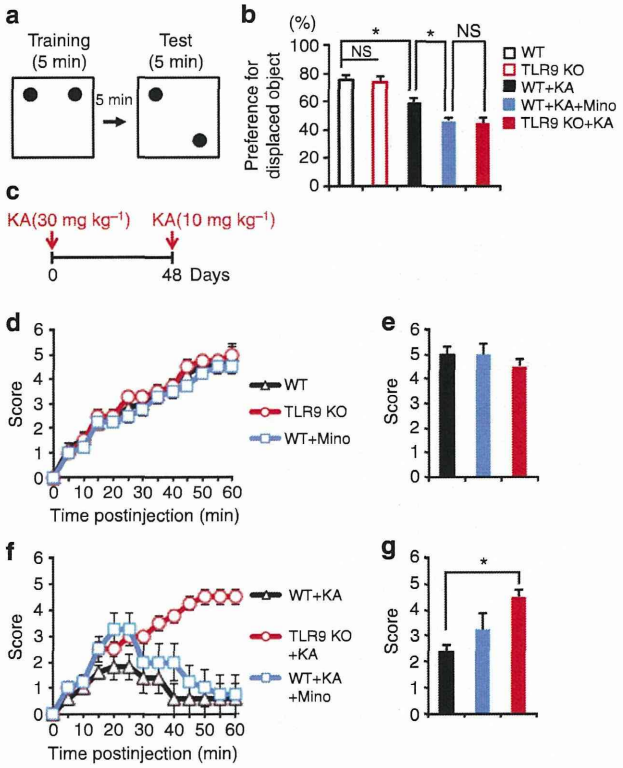

Figure 5 | TLR9 deficiency worsens seizure-induced behavioural impairments. (**a**) Schematic paradigm of place recognition test. Five minutes after training phase, mice were allowed to explore two objects one of which was displaced to different location from the original location. (**b**) KA-treated WT mice did not show much preference for the displaced object compared with untreated WT mice. This cognitive decline was exacerbated in TLR9 KO mice. KA-treated WT mice that received minocycline treatment showed the similar level of preference for the displaced object as KA-treated TLR9-KO mice did. Each group has eight mice. NS means not significant ($P>0.05$). *$P<0.05$ by analysis of variance (ANOVA) with Tukey *post-hoc* tests. (**c**) Experimental scheme for examining recurrent seizure severity. All mice were administrated with KA (10 mg kg^{-1}) 48 days after first KA injection (30 mg kg^{-1}). (**d**) Seizure response over time in WT, TLR9 KO and minocycline-treated WT mice following the first KA injection (30 mg kg^{-1}) ($n=8$ animals). For each 5-min interval, the highest level of seizure activity was scored using previously described scale (see Methods). (**e**) The maximum score of each mouse group during the 60-min trial in **d**. (**f**) Seizure response over time in WT mice, TLR9 KO mice and minocycline-treated WT mice following KA injection (10 mg kg^{-1}) 48 days after first KA injection ($n=8$ animals). (**g**) The maximum score of each mouse group during the 60-min trial in **f**. *$P<0.01$ by ANOVA with Tukey *post-hoc* tests.

the inhibition of aberrant neurogenesis was less effective in minocycline-treated WT mice than in untreated WT mice. Taken together, these results suggest that TLR9 signalling attenuates seizure-induced cognitive decline and recurrent seizure severity.

Degenerating neuron-derived DNA activates TLR9 signalling. Finally, we addressed the possibility that an endogenous cell-derived ligand activates TLR9 signalling in microglia after seizure. Increasing evidence indicates that, in addition to detection of PAMPs, TLRs contribute to the detection of damage to the CNS by recognizing endogenous DAMPs released from dying or degenerating cells[15,16,27]. As we have shown previously[18], seizure causes neuronal degeneration in the DG. We collected CM from

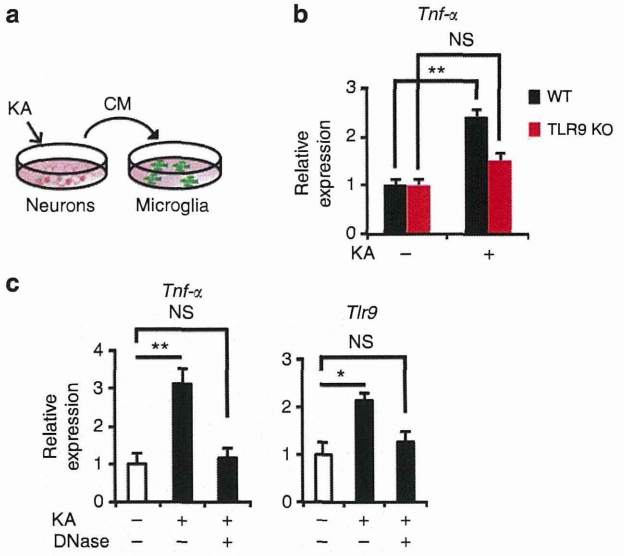

Figure 6 | Degenerating neuron-derived DNA activates TLR9 signalling. (**a**) Experimental scheme for the identification of an endogenous ligand for TLR9 expressed in microglia. (**b**) qRT-PCR analyses of *Tnf-α* levels in microglia from WT and TLR9 KO mice 12 h after incubation with CM from KA-treated or -untreated neurons. TLR9 KO microglia failed to induce *Tnf-α* expression in response to CM from KA-treated neurons ($n=4$ experiments). (**c**) qRT-PCR analyses of *Tnf-α* expression levels in microglia from WT mice 12 h after incubation with DNase-pretreated CM from KA-treated neurons ($n=5$ experiments). NS means not significant ($P>0.05$). *$P<0.05$ and **$P<0.01$ by ANOVA with Tukey *post-hoc* tests.

hippocampal neurons stimulated with KA, and cultured primary microglia in its presence for 12 h (Fig. 6a). We found that the *Tnf-α* expression level in primary WT microglia was increased by the CM of KA-treated neurons. In contrast, the CM failed to induce *Tnf-α* expression in TLR9-KO microglia (Fig. 6b). When we pretreated the CM from KA-treated neurons with DNase, the CM-induced elevation of *Tnf-α* expression in primary microglia was abolished (Fig. 6c). These data suggest that DNA derived from degenerating neurons activates TLR9 signalling in microglia as an endogenous ligand. Moreover, we observed that the CM of KA-treated neurons upregulated the expression of *Tlr9* in primary microglia, indicating the existence of a positive feedback loop to enhance TLR9 signalling in microglia (Fig. 6c). CM-induced *Tlr9* expression was also severely compromised by pretreatment with DNase.

The TLR9 signalling pathway is known to activate NF-κB, which controls the expression of inflammatory cytokine genes[28]. We examined whether CM from degenerating neurons induces NF-κB activation in microglia via TLR9. When we cultured microglia with CM derived from KA-stimulated hippocampal neurons, p65 protein, a subunit of the NF-κB complex, translocated into the nucleus, indicating that the CM can indeed activate NF-κB in microglia (Supplementary Fig. 13a,b). This activation was abolished by DNase or TLR9 inhibitor (ODN2088) treatment (Supplementary Fig. 13a,b). These data suggest that DNA derived from degenerating neurons evokes NF-κB activation in microglia via TLR9.

Discussion

TLR9 was initially identified as a receptor that recognizes microbial DNA[29], but current research has shown that TLR9 can sense self-DNA as a DAMP[30], and it appears to be involved in numerous immune processes and autoimmune diseases[14].